BIFURCATION OF RELATIVE EQUILIBRIA GENERATED BY A CIRCULAR VORTEX PATH IN A CIRCULAR DOMAIN

DAVID ROJAS*

Departament d'Informàtica, Matemàtica Aplicada i Estadística
Universitat de Girona, 17003 Girona, Spain

PEDRO J. TORRES

Departamento de Matemática Aplicada
Universidad de Granada, 18071 Granada, Spain

ABSTRACT. We study the passive particle transport generated by a circular vortex path in a 2D ideal flow confined in a circular domain. Taking the strength and angular velocity of the vortex path as main parameters, the bifurcation scheme of relative equilibria is identified. For a perturbed path, an infinite number of orbits around the centers are persistent, giving rise to periodic solutions with zero winding number.

1. **Introduction.** The passive particle transport in a 2D incompressible inviscid flow with prescribed vorticity is a research topic of the highest relevance in Fluid Dynamics [2, 8, 10]. In the Lagrangian formulation, the advection of single particles is ruled by a Hamiltonian system where the stream function plays the role of the Hamiltonian. In this paper, we consider the dynamics induced in an ideal flow confined in a circular domain of radius R under the action of a prescribed T-periodic vortex path. Such dynamics model the stirring process of an agitator plunged into a fluid inside a cylindrical tank free surface. The main interest of this model is to investigate the amount of fluid that actually mix and how the path of the vortex affects stirring. We refer to [1, 3, 4, 6] and references therein for more information on the model and its historical overview in the literature.

Let $B_R \subset \mathbb{R}^2$ be the open ball of center $(0,0)$ and radius R, and consider a T-periodic vortex path given by $z : \mathbb{R} \to B_R$. Then, the stream function of the fluid confined in B_R and under the action of the vortex is given by

$$\Psi(t,\zeta) = \frac{\Gamma}{2\pi}\left(\ln|\zeta - z(t)| - \ln\left|\zeta - \frac{R^2}{|z(t)|^2}z(t)\right|\right).$$

Here, Γ is the strength or charge of the vortex, and its sign gives the sense of rotation. In this function, the first term accounts for the vortex action, whereas the

second term models the influence of the solid circular boundary. It is useful to see ζ as a complex variable, then the corresponding Hamiltonian system is

$$\dot{\zeta^*} = \frac{\Gamma}{2\pi i} \left(\frac{1}{\zeta - z(t)} - \frac{1}{\zeta - \frac{R^2}{|z(t)|^2} z(t)} \right), \tag{1}$$

where the asterisk means the complex conjugate.

In the related literature, $z(t)$ is called the *stirring protocol*. When it is constant, then Ψ is a conserved quantity and all the particles rotate around the vortex in circular trajectories. In particular, the model does not mix appropiately. When $z(t)$ is time-dependent, then the Hamiltonian ceases to be a conserved quantity and one must in general expect to observe chaotic particle motion. In this direction, Aref [1] proves the existence of chaotic regions in the case when the protocol $z(t)$ is piece-wise constant (also known as blinking protocol) by showing that the Poincaré map is semiconjugate to the Bernoulli shift on two symbols. In particular, the blinking protocol produce an efficient mixing.

In [3], it is proved that any smooth stirring protocol $z(t)$ induces an infinite number of periodic trajectories rotating around the vortex (non-zero winding number). A natural question is to try to identify the stirring protocols that generate periodic trajectories with zero winding number, that is, particles moving periodically but not rotating around the vortex. This question was posed explicitly as an open problem in [9, Section 7.3]. The identification of periodic solutions of zero winding number is relevant in the interpretation of the model as a stirring problem. Indeed, in the case of the existence of stable solutions, the stability region conforms a confined portion of fluid that will not mix with the fluid around the vortex.

Our intention is to advance on the comprehension of this problem by analyzing the family of circular protocols $z(t) = r_0 \exp(i\theta_0 t)$. In this case, the change to a corotating frame $\zeta(t) = \eta(t) \exp(i\theta_0 t)$ transforms equation (1) into the autonomous system

$$\dot{\eta}^* = i\theta_0 \eta^* + \frac{\Gamma}{2\pi i} \left(\frac{1}{\eta - r_0} - \frac{1}{\eta - \frac{R^2}{r_0}} \right). \tag{2}$$

The Hamiltonian structure is preserved, so the streamlines are just the level curves of the corresponding Hamiltonian, which is indeed a conserved quantity. In [6], the authors study the case when the stirring protocol moves according with the passive motion of the fluid (free vortex). That is, the trajectories of the vortex are circles with radii r_0 and angular speed $\theta_0 = \frac{\Gamma}{2\pi} \frac{1}{R^2 - r_0^2}$. In this case, the phase portrait of the disk consists on a heteroclinic connection between two points on the boundary of B_R separating the vortex from a center generated by the passive fluid (see Figure 1b.) The authors evidence regions of chaotic motion via Melnikov method due to the transverse crossing of the stable and unstable manifolds of the heteroclinic orbit once the radius of the stirring protocol is perturbed by a 2π-periodic function.

Our first contribution in this direction is to classify all possible phase portraits for all circular stirring protocols. That is, we will consider $\theta_0 \in \mathbb{R}$ as a free parameter. By a complete bifurcation analysis of the relative equilibria, performed in Section 2, setting $\phi_0 := \frac{2\pi R^2 \theta_0}{\Gamma}$ and $\rho_0 := \frac{r_0}{R}$, we obtain five regions in the parameter space $(\phi_0, \rho_0) \in \mathbb{R} \times (0, 1)$ with phase portraits as shown in Figures 1a to 1e divided by four codimension one curves with phase portraits as shown in Figures 1f to 1h (the curve $\phi_0 = 0$ correspond to the constant stirring protocol.) In particular, the center inside
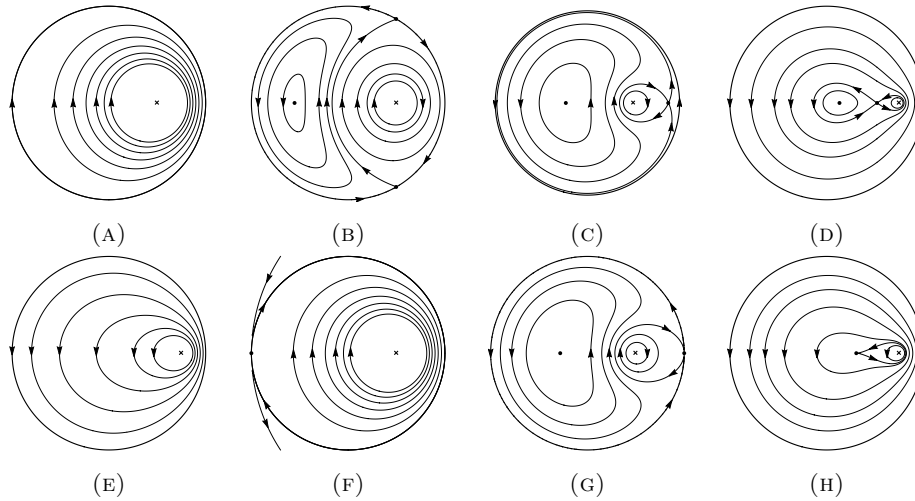
FIGURE 1. Phase portrait of system (3) depending on the parameters according to Theorem 2.1.

the ball B_R is not always present and there are no periodic orbits with zero winding number at least in the integrable scenario. In Section 3 we consider the case when the radius of the stirring protocol is perturbed by a T-periodic function. As in [6] the natural scenario is that, in the cases that homoclinic or heteroclinic orbits appear separating the vortex and the center, such stable and unstable manifolds generically intersect transversally giving rise to chaotic regions. Our second contribution is an analytic proof showing that, under small periodic perturbations of the radius of $z(t)$, there are still periodic trajectories surrounding a certain perturbed critical point and giving rise to periodic orbits with zero winding number. Consequently, in the terminology of Fluid Dynamics the model turns to be a not efficient stirring process.

2. **Phase portrait and bifurcation analysis.** This section is devoted to the bifurcation analysis of the phase portrait of system (2). Working on Cartesian coordinates, the streamlines are level curves of the Hamiltonian function

$$\Psi(x,y) = -\frac{\theta_0}{2}(x^2+y^2) + \frac{\Gamma}{2\pi}\ln\sqrt{\frac{(x-r_0)^2+y^2}{(x-\frac{R^2}{r_0})^2+y^2}}.$$

Here $(R,\Gamma,\theta_0) \in (0,+\infty) \times (\mathbb{R} \setminus \{0\})^2$ and $r_0 \in (0,R)$. From now on, for the sake of further simplicity, we denote

$$a(x) := a(x,r_0) = x - r_0, \ b(x) := b(x,R,r_0) = x - \frac{R^2}{r_0} \text{ and } c := \frac{\Gamma}{2\pi\theta_0}.$$

Thus, system (2) can be written in the (x,y)-variables as

$$\begin{cases} \dot{x} = \dfrac{\partial\Psi}{\partial y} = -\theta_0 y + c\theta_0 y\left(\dfrac{1}{a(x)^2+y^2} - \dfrac{1}{b(x)^2+y^2}\right), \\ \dot{y} = -\dfrac{\partial\Psi}{\partial x} = \theta_0 x - c\theta_0\left(\dfrac{a(x)}{a(x)^2+y^2} - \dfrac{b(x)}{b(x)^2+y^2}\right). \end{cases} \tag{3}$$

Let $D_R \subset \mathbb{R}^2$ be the closed ball of center $(0,0)$ and radius R. It is an immediate calculation to show that D_R is invariant by the flow of system (3). Next result deals with the phase portrait of the system on D_R. It will be shown that the position r_0 and angular velocity θ_0 of the vortex path are the main parameters on the system, whereas the remaining ones can be normalized. To this end, and for the sake of simplicity on the statement, we set $\rho_0 := \frac{r_0}{R}$ and $\phi_0 := \frac{R^2}{c} = \frac{2\pi R^2 \theta_0}{\Gamma}$. Thus, the parameter space of system (3) turns $\Lambda := \{(\rho_0, \phi_0) \in \mathbb{R}^2 : 0 < \rho_0 < 1 \text{ and } \phi_0 \neq 0\}$. Moreover, let us define

$$f(\rho_0, \phi_0) := 27\rho_0^2(\rho_0^2 - 1) + \phi_0 \left(2 - 3\rho_0^2 - 3\rho_0^4 + 2\rho_0^6 - 2(1 - \rho_0^2 + \rho_0^4)^{\frac{3}{2}} \right),$$

and

$$\mathcal{B} := \left\{ (\rho_0, \phi_0) \in \Lambda : \phi_0 f(\rho_0, \phi_0) \left(\rho_0 - \frac{1 - \phi_0}{1 + \phi_0} \right) \left(\rho_0 - \frac{\phi_0 - 1}{1 + \phi_0} \right) = 0 \right\}.$$

We claim that there is no $\rho_0 \in (0,1)$ such that

$$2 - 3\rho_0^2 - 3\rho_0^4 + 2\rho_0^6 - 2(1 - \rho_0^2 + \rho_0^4)^{\frac{3}{2}} = 0.$$

Indeed, the previous equality is equivalent to

$$-27\rho_0^4(\rho_0 - 1)^2(\rho_0 + 1)^2 = 0$$

by means of elementary algebraic manipulations. Therefore, the curve $\mathcal{B}$ is the union of three curves, namely

$$C_1 := \{(\rho_0, \phi_0) \in \Lambda : \rho_0 = \tfrac{1 - \phi_0}{1 + \phi_0}\},$$
$$C_2 := \{(\rho_0, \phi_0) \in \Lambda : \rho_0 = \tfrac{\phi_0 - 1}{1 + \phi_0}\},$$
$$C_3 := \{(\rho_0, \phi_0) \in \Lambda : f(\rho_0, \phi_0) = 0\},$$

and splits the parameter space Λ into five connected components, namely $\mathcal{R}_i$, $i = 1, \ldots, 5$, according with Figure 2.

Theorem 2.1. *Let $(\rho_0, \phi_0) \in \Lambda$. The set $\Lambda \setminus \mathcal{B}$ corresponds to regular parameters of system* (3)*. On each connected component, the phase portrait is the following:*

(a) *If $(\rho_0, \phi_0) \in \mathcal{R}_1$ then the dynamics on D_R is a global vortex at $(r_0, 0)$ (see Figure 1a).*

(b) *If $(\rho_0, \phi_0) \in \mathcal{R}_2$ then the system has a vortex at $(r_0, 0)$, a center at $(x_c^*, 0)$ with $x_c^* \in (-R, 0)$ and two hyperbolic saddles $(x_s^*, \pm y_s^*)$ at ∂D_R with a saddle connection inside D_R (see Figure 1b).*

(c) *If $(\rho_0, \phi_0) \in \mathcal{R}_3$ then the system has a vortex at $(r_0, 0)$, a center at $(x_c^*, 0)$ with $x_c^* \in (-R, 0)$ and a hyperbolic saddle at $(x_s^*, 0)$ with $x_s^* \in (r_0, R)$ (see Figure 1c).*

(d) *If $(\rho_0, \phi_0) \in \mathcal{R}_4$ then the system has a vortex at $(r_0, 0)$, a center $(x_c^*, 0)$ and a hyperbolic saddle $(x_s^*, 0)$ satisfying $0 < x_c^* < x_s^* < r_0$ (see Figure 1d).*

(e) *If $(\rho_0, \phi_0) \in \mathcal{R}_5$ then the dynamics on D_R is a global vortex at $(r_0, 0)$ (see Figure 1e).*

Moreover, the set $\mathcal{B}$ corresponds to bifurcation parameters of system (3)*. On each curve the phase portrait is the following:*

(f) *If $(\rho_0, \phi_0) \in C_1$ then the system has a vortex at $(r_0, 0)$ and a degenerated saddle at $(-R, 0)$ (see Figure 1f).*

(g) *If $(\rho_0, \phi_0) \in C_2$ then the system has a vortex at $(r_0, 0)$, a center at $(x_c^*, 0)$ with $x_c^* \in (-R, 0)$ and a degenerated saddle at $(R, 0)$ (see Figure 1g).*
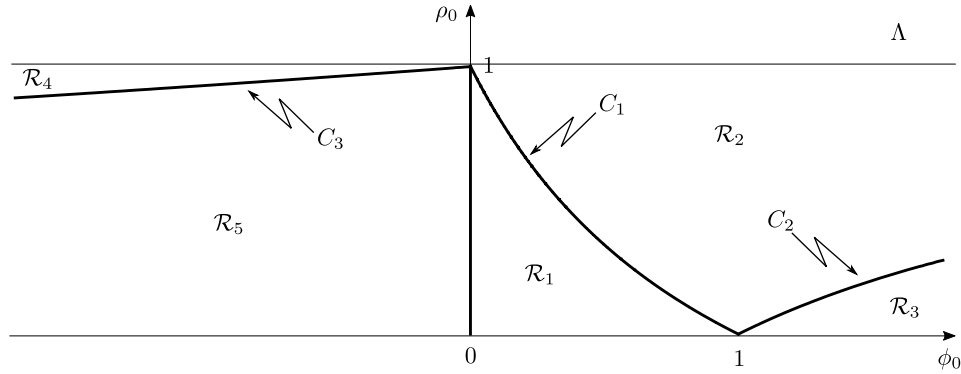
FIGURE 2. Bifurcation diagram of the phase-portrait of system (3) on D_R. The bold curve corresponds to bifurcation parameters $\mathcal{B}$, whereas the remaining ones correspond to regular parameters. In Theorem 2.1 the phase portrait at each region is given.

(h) If $(\rho_0, \phi_0) \in C_3$ then the system has a vortex at $(r_0, 0)$ and a cusp at $(x_p^*, 0)$ (see Figure 1h), where

$$x_p^* := x_p^*(R, r_0) = \frac{R^2 + r_0^2 - \sqrt{R^4 - R^2 r_0^2 + r_0^4}}{3r_0}.$$

Proof. For the sake of simplicity we first begin the proof by showing that the only critical points in D_R that do not lie on the line $\{y = 0\}$ are the hyperbolic saddles $(x_s^*, \pm y_s^*)$ at ∂D_R of case (b) on the statement. To this end, assuming $y \neq 0$, from equations in (3) we have that $\dot{x} = 0$ if and only if

$$-1 + c\left(\frac{1}{a(x)^2 + y^2} - \frac{1}{b(x)^2 + y^2}\right) = 0.$$

Since $a(x)^2 < b(x)^2$ for all $x < R$, if $\phi_0 < 0$ then $c < 0$ and so the left-hand side of the previous equality is negative. Then assume $\phi_0 > 0$. In this case, $\dot{x} = 0$ if and only if

$$y^2 = -\frac{1}{2}(a(x)^2 + b(x)^2) + \frac{1}{2}\sqrt{(b(x)^2 - a(x)^2)(4c + b(x)^2 - a(x)^2)}.$$

Substituting the previous equality on the expression of $\dot{y}$ in (3) and equaling to zero one gets the equation

$$\frac{(2x - a(x) - b(x))(a(x) + b(x)) + \sqrt{(b(x)^2 - a(x)^2)(4c + b(x)^2 - a(x)^2)}}{2(a(x) + b(x))} = 0.$$

Thus, using that $a(x) = x - r_0$ and $b(x) = x - \frac{R^2}{r_0}$, the previous equation has the unique solution

$$x_s^* = \frac{R^2 + r_0^2}{2r_0} - \frac{c}{2r_0}\left(1 - \frac{r_0^2}{R^2}\right)$$

and so

$$(y_s^*)^2 = \frac{1}{4}\left(\frac{2(c^2 + R^4)}{R^2} - \frac{(c - R^2)^2}{r_0^2} - \frac{(c + R^2)^2 r_0^2}{R^4}\right).$$

It is a computation to show that $x_s^* \in (-R, R)$ if and only if $\rho_0 > \max\{\frac{1-\phi_0}{1+\phi_0}, \frac{\phi_0-1}{1+\phi_0}\}$ (that is, $(\rho_0, \phi_0) \in \mathcal{R}_2$) and $(x_s^*)^2 + (y_s^*)^2 = R^2$. It is only remaining to prove that $(x_s^*, \pm y_s^*)$ are hyperbolic saddles. This can be done evaluating the previous expression of the points $(x_s^*, \pm y_s^*)$ on the Jacobian matrix of system (3). In the case of (x_s^*, y_s^*) the determinant of the Jacobian matrix is

$$\det(DX(x_s^*, y_s^*)) = \frac{(cR - R^3 - (c + R^2)r_0)(cR - R^3 + (c + R^2)r_0)\theta_0^2}{c^2(R^2 - r_0^2)}$$

which is negative if and only if $\rho_0 > \max\{\frac{1-\phi_0}{1+\phi_0}, \frac{\phi_0-1}{1+\phi_0}\}$. Then, (x_s^*, y_s^*) is a hyperbolic saddle. The same argument is valid for $(x_s^*, -y_s^*)$. Moreover, since ∂D_R is an invariant curve of system (3) and $(x_s^*, y_s^*) \in \partial D_R$, then ∂D_R is the stable manifold of one saddle (and unstable of the other). The corresponding unstable (stable) manifold cuts transversally the disk of radius R due to the hyperbolicity of the saddles and so the connection between the saddles follows by Poincaré-Bendixon's theorem.

The previous argument shows that out of case (b) on the statement, all the critical points of system (3) lie on $\{y = 0\}$. Let us prove now the remaining cases of the result. Let us first consider $\phi_0 > 0$. This corresponds to the statements $(a) - (c)$ and $(f) - (g)$. We can assume with no loss of generality that $\theta_0 > 0$ and $\Gamma > 0$. The case with $\theta_0 < 0$ and $\Gamma < 0$ follows by reversion of time. Notice that the hypothesis $\phi_0 > 0$ implies $c > 0$. System (3) has a critical point at $(x^*, 0)$ inside the disk of radius R if and only if the function

$$F(x) := \theta_0 \left(x - c \left(\frac{1}{a(x)} - \frac{1}{b(x)} \right) \right)$$

satisfies $F(x^*) = 0$ for some $x^* \in (-R, R)$. Multiplying by $a(x)b(x)$ the previous condition turns into $F(x^*)a(x^*)b(x^*) = 0$. We point out that, on account of the expressions of $a(x)$ and $b(x)$, the previous two conditions are equivalent if $x^* \notin \{r_0, \frac{R^2}{r_0}\}$ (those correspond to singularities on the Hamiltonian function and so no critical points). Thus, system (3) has a critical point at $(x^*, 0)$ in D_R if and only if

$$x^* a(x^*)b(x^*) = c\left(r_0 - \frac{R^2}{r_0}\right) =: \lambda = \lambda(r_0, R, c). \tag{4}$$

Notice that, since $\phi_0 > 0$ then $\lambda < 0$. The cubic polynomial $P(x) := xa(x)b(x)$ has zeros at $x = 0$, $x = r_0$ and $x = \frac{R^2}{r_0}$. $P(x)$ is negative if $x \in (-\infty, 0) \cup (r_0, R^2/r_0)$ and it is positive if $x \in (0, r_0) \cup (R^2/r_0, +\infty)$, and the local maximum and minimum are, respectively,

$$x_M = \frac{R^2 + r_0^2 - \sqrt{R^4 - R^2 r_0^2 + r_0^4}}{3r_0} \quad \text{and} \quad x_m = \frac{R^2 + r_0^2 + \sqrt{R^4 - R^2 r_0^2 + r_0^4}}{3r_0}.$$

Moreover, since $\phi_0 > 0$ then $\lambda = \lambda(r_0, R, c)$ varies from zero to $-\infty$. Thus $P(x) - \lambda = 0$ has always a solution $x^* \in (-\infty, 0)$, it has a double solution $x^* = x_m$ if $P(x_m) = \lambda$ and two solutions in $(r_0, R^2/r_0)$ if $P(x_m) < \lambda$. Let us study when these solutions correspond to critical points in D_R. To this end, we define $Q(u) :=$

$\frac{1}{R^3}(P(Ru) - \lambda)$. Elementary algebraic manipulations show that

$$0 < \frac{x_M}{R} < \frac{1 + \rho_0^2 - \sqrt{(1 - \rho_0^2)^2 + \rho_0^2}}{3\rho_0} < \rho_0 < 1 < \frac{x_m}{R},$$

$$Q(1) = \frac{(1 - \rho_0)(\phi_0 + 1)}{\phi_0 \rho_0} \left(\rho_0 - \frac{\phi_0 - 1}{1 + \phi_0} \right),$$

$$Q(-1) = \frac{-(1 + \rho_0)(\phi_0 + 1)}{\phi_0 \rho_0} \left(\rho_0 - \frac{1 - \phi_0}{1 + \phi_0} \right),$$

$$Q(0) = Q(\rho_0) = \frac{1 - \rho_0^2}{\phi_0 \rho_0} > 0.$$

We point out that since $x_m > R$ then at most two zero of $P(x) - \lambda$ lie in $(-R, R)$. By the second equality above we have that $P(R) - \lambda > 0$ if $\rho_0 > \frac{\phi_0 - 1}{1 + \phi_0}$, that $P(R) - \lambda = 0$ if $\rho_0 = \frac{\phi_0 - 1}{1 + \phi_0}$ and $P(R) - \lambda < 0$ if $\rho_0 < \frac{\phi_0 - 1}{1 + \phi_0}$. By the third equality above we have that $P(-R) - \lambda > 0$ if $\rho_0 < \frac{1 - \phi_0}{1 + \phi_0}$, that $P(-R) - \lambda = 0$ if $\rho_0 = \frac{1 - \phi_0}{1 + \phi_0}$ and that $P(-R) - \lambda < 0$ if $\rho_0 > \frac{1 - \phi_0}{1 + \phi_0}$. Thus, if $(\rho_0, \phi_0) \in \mathcal{R}_1$ no roots of $P(x) - \lambda$ are inside $[-R, R]$ and so the result in (a) holds. If $(\rho_0, \phi_0) \in C_1$ the unique zero of $P(x) - \lambda$ in $[-R, R]$ is $x = -R$. This correspond to a critical point of system (3) at $(-R, 0)$. Moreover, it is a degenerated saddle since ∂D_R is an invariant curve of system (3) so (f) is proved. If $(\rho_0, \phi_0) \in \mathcal{R}_2$ then $P(x) - \lambda$ has only one zero $x_C^* \in (-R, 0)$. Then, on account of the previous discussion about the hyperbolic saddles $(x_s^*, \pm y_s*)$ on ∂D_R, result in (b) is proved. If $(\rho_0, \phi_0) \in C_2$ then $P(x) - \lambda$ has two zeros: $x = x_c^* \in (-R, 0)$ and $x = R$. The critical point $(R, 0)$ corresponds to a degenerated saddle since ∂D_R is an invariant curve of system (3). Then (g) holds. Finally, if $(\rho_0, \phi_0) \in \mathcal{R}_3$ then $P(x) - \lambda$ has two zeros: $x = x_c^* \in (-R, 0)$ and $x = x_s^* \in (r_0, R)$. In order to end with the case $\phi_0 > 0$ it only remains to prove that x_c^* and x_s^* are a center and a hyperbolic saddle, respectively.

The Jacobian matrix associated to system (3) with $y = 0$ is given by

$$DX(x, 0) = \begin{pmatrix} 0 & \theta_0 \left(-1 + c \left(\frac{1}{a(x)^2} - \frac{1}{b(x)^2} \right) \right) \\ \theta_0 \left(1 + c \left(\frac{1}{a(x)^2} - \frac{1}{b(x)^2} \right) \right) & 0 \end{pmatrix}. \tag{5}$$

Notice that $\theta_0 \left(1 + c \left(\frac{1}{a(x)^2} - \frac{1}{b(x)^2} \right) \right) > 0$ for all $x \in (-R, R)$. Furthermore, setting $x = x^*$ a critical point of (3), we have

$$c \left(\frac{1}{a(x^*)^2} - \frac{1}{b(x^*)^2} \right) - 1 = x^* \left(\frac{1}{a(x^*)} + \frac{1}{b(x^*)} \right) - 1$$

$$= \frac{(x^*)^2 - R^2}{(x^* - r_0)(x^* - \frac{R^2}{r_0})},$$

where we used $F(x^*) = 0$ on the first equality and the expressions of $a(x)$ and $b(x)$ on the second. Thus

$$DX(x^*, 0) = \begin{pmatrix} 0 & \theta_0 \frac{(x^*)^2 - R^2}{(x^* - r_0)(x^* - \frac{R^2}{r_0})} \\ \theta_0 \left(2 + \frac{(x^*)^2 - R^2}{(x^* - r_0)(x^* - \frac{R^2}{r_0})} \right) & 0 \end{pmatrix}. \tag{6}$$

Consequently, taking $x^* = x_c^* \in (-R, 0)$ we have $(x_c^*)^2 - R^2 < 0$ and $(x_c^* - r_0)(x_c^* - R^2/r_0) > 0$. Therefore $\frac{(x_c^*)^2 - R^2}{(x_c^* - r_0)(x_c^* - R^2/r_0)} < 0$ and so $\det(DX(x_c^*, 0)) > 0$. This implies that $(x_c^*, 0)$ is a center. On the other hand, taking $x^* = x_s^* \in (r_0, R)$, $\frac{(x_s^*)^2 - R^2}{(x_s^* - r_0)(x_s^* - R^2/r_0)} > 0$ and so $\det(DX(x_s^*, 0)) < 0$. This implies that $(x_s^*, 0)$ is a hyperbolic saddle. This ends with the proof of statements (a), (b), (c), (f) and (g).

Let us now consider the case $\phi_0 < 0$. This corresponds to statements (d), (e) and (h). In this situation we can assume with no loss of generality that $\theta_0 > 0$ and $\Gamma < 0$. The opposite case follows by reversion of time. Notice that the hypothesis $\phi_0 < 0$ implies $c < 0$. Consequently, on account of the equation (3) critical points can only belong to $\{(x, y) \in \mathbb{R}^2 : y = 0\}$. Similarly as before, system (3) has a critical point at $(x^*, 0)$ inside the disk of radius R if and only if (4) is satisfied. Notice that, since $\phi_0 < 0$, in this case $\lambda = \lambda(r_0, R, c)$ varies from zero to $+\infty$. Thus, on account of $R < R^2/r_0$, if λ stays above of the maxima of $P(x)$ inside $(0, r_0)$ then $P(x) - \lambda = 0$ has a unique zero which is larger than R. This happens when $f(\rho_0, \phi_0) < 0$. If $f(\rho_0, \phi_0) = 0$ then the maximum of $P(x)$ inside $(0, r_0)$ contact λ and gives the cusp $(x_p^*, 0)$ with $x_p^* = x_M$. Finally, if $f(\rho_0, \phi_0) > 0$ then the maximum of $P(x)$ is greater than λ and so $P(x) - \lambda$ has two real roots inside $(0, r_0)$: namely x_c^* and x_s^*, satisfying $0 < x_c^* < x_M < x_s^* < r_0$. It only remains to prove the stability of such critical points. This follows from the expression in (5) of the Jacobian matrix associated to system (3) with $y = 0$. We point out that, since $a(x)^2 < b(x)^2$ for all $x \in (0, r_0)$ and $c < 0$, we have

$$\theta_0 \left(-1 + c \left(\frac{1}{a(x)^2} - \frac{1}{b(x)^2} \right) \right) < 0.$$

Moreover, setting $x = x^*$ a critical point of system (3), on account of $F(x^*) = 0$ we have

$$1 + c \left(\frac{1}{a(x^*)^2} - \frac{1}{b(x^*)^2} \right) = 2 + \frac{(x^*)^2 - R^2}{(x^* - r_0)(x^* - \frac{R^2}{r_0})}$$

$$= \frac{3r_0(x^*)^2 - 2(R^2 + r_0^2)x^* + R^2 r_0}{(r_0 - x^*)(R^2 - r_0 x^*)}.$$

The previous expression is positive if $x^* \in (0, x_M)$ and it is negative if $x^* \in (x_M, r_0)$. This proves that x_c^* is a center and x_s^* is a hyperbolic saddle and ends with the proof of (d), (e) and (h). $\qquad \square$

3. **Periodic perturbations and local continuation of periodic orbits.** Given an autonomous planar Hamiltonian system

$$\dot{\eta} = J \nabla \mathcal{H}(\eta), \tag{7}$$

it is interesting to look for the existence of periodic solutions of the non-autonomous planar Hamiltonian system

$$\dot{\eta} = J \nabla H(t, \eta; \epsilon), \tag{8}$$

which are small T-periodic perturbations of (7) meaning that $H(t, \eta; 0) \equiv \mathcal{H}(\eta)$. A. Fonda, M. Sabatini and F. Zanolin prove in [5] that under the hypothesis of the existence of a non-isochronous period annulus for the autonomous Hamiltonian system and some regularity conditions on $H(t, \eta; \epsilon)$ such periodic orbits exist.

More precisely, consider $\mathcal{H} : \mathcal{A} \to \mathbb{R}$ twice continuously differentiable and $\mathcal{A} \subseteq \mathbb{R}^2$ a period annulus such that the inner and outer components of its boundary are Jordan curves. Assume that $\mathcal{A}$ is not isochronous, that is the period of the periodic

orbits in $\mathcal{A}$ covers an interval $[\mathcal{T}_{\min}, \mathcal{T}_{\max}]$, with $\mathcal{T}_{\min} < \mathcal{T}_{\max}$. Then consider $H :$ $\mathbb{R} \times \mathcal{A} \times (0, \epsilon_0) \to \mathbb{R}$, whose gradient with respect to the second variable, denoted by $\nabla H(t, \eta; \epsilon)$, is continuous in $(t, \eta; \epsilon)$, locally Lipschitz continuous in η and T-periodic in t for some $T > 0$. Under these assumptions, the authors in [5] prove the following result:

Theorem 3.1 (Fonda, Sabatini and Zanolin). *Given two positive integers m and n satisfying*

$$\mathcal{T}_{\min} < \frac{mT}{n} < \mathcal{T}_{\max}, \tag{9}$$

there is an $\bar{\epsilon} > 0$ such that, if $|\epsilon| \leq \bar{\epsilon}$, then system (8) has at least two mT-periodic solutions, whose orbits are contained in $\mathcal{A}$, which make exactly n rotations around the origin in the period time mT.

The authors also emphasize the following immediate consequence:

Corollary 1. *For any positive integer N there is a $\bar{\epsilon}_N > 0$ such that, if $|\epsilon| < \bar{\epsilon}_N$, then system (8) has at least N periodic solutions, whose orbits are contained in $\mathcal{A}$.*

Our purpose in this section is to illustrate this situation in the case when system (3) has a non-degenerated center inside D_R. This occurs for parameters $(\rho_0, \phi_0) \in \mathcal{R}_2 \cup \mathcal{R}_3 \cup \mathcal{R}_4$, corresponding to the phase portraits (b), (c) and (d) in Figure 1 and Theorem 2.1. Let us denote by $\mathscr{P}$ the period annulus of the center. The inner boundary of $\mathscr{P}$ is the center itself, namely p, whereas the outer boundary of $\mathscr{P}$ is formed by saddle connections. In both cases the outer boundary has critical points so it is clear that the period function tends to infinity as the orbits approach the outer boundary. Particularly, the center is not isochronous. Next result states the period of the linearized center.

Lemma 3.2. *Let $(\rho_0, \phi_0) \in \mathcal{R}_2 \cup \mathcal{R}_3 \cup \mathcal{R}_4$ and let $p = (x, 0)$ be the non-degenerated center of system (3). Then the period of the associated linearized system at p is*

$$T_0(x) = \frac{2\pi}{\sqrt{\theta_0^2 \nu(\frac{x}{R})(2 + \nu(\frac{x}{R}))}}$$

where $\nu(x) := \dfrac{x^2 - 1}{(x - \rho_0)(x - \frac{1}{\rho_0})}$.

Proof. From the expression of the Jacobian matrix of the system in (6) we have that the eigenvalues associated to the center are

$$\lambda_{\pm} = \pm \omega i = \pm \sqrt{\theta_0^2 \frac{x^2 - R^2}{(x - r_0)(x - \frac{R^2}{r_0})} \left(2 + \frac{(x^2 - R^2)}{(x - r_0)(x - \frac{R^2}{r_0})}\right)} i$$

where ω denotes the frequency of the linearized center. Thus, setting $\rho_0 = \frac{r_0}{R}$, and using that the period of the linearized center is $T_0 = \frac{2\pi}{\omega}$ the result holds. $\square$

Let us now consider the periodically perturbed stirring protocol

$$z_\epsilon(t) = r_\epsilon(t) \exp(i\theta_0 t)$$

on system (1) where $r_\epsilon(t)$ is a smooth T-periodic perturbation of r_0. More concretely, $r_\epsilon(t) = r_0 + \epsilon f(t) + g(t; \epsilon)$ with f and $g(\cdot; \epsilon)$ T-periodic analytic functions and $g(t; \epsilon)$ tending to zero uniformly on $t \in \mathbb{R}$ as ϵ tends to zero. The same change

to a corotating frame than the presented at the beginning of this paper transforms (1) into a periodic Hamiltonian system with Hamiltonian function

$$\Psi(t, x, y; \epsilon) = -\frac{\theta_0}{2}(x^2 + y^2) + \frac{\Gamma}{2\pi} \ln \sqrt{\frac{(x - r_\epsilon(t))^2 + y^2}{(x - \frac{R^2}{r_\epsilon(t)})^2 + y^2}}. \tag{10}$$

Theorem 3.3. *Let $(\rho_0, \phi_0) \in \mathcal{R}_2 \cup \mathcal{R}_3 \cup \mathcal{R}_4$. For any positive integer N there is a $\bar{\epsilon}_N > 0$ such that, if $|\epsilon| < \bar{\epsilon}_N$, then the Hamiltonian system $\dot{u} = J\nabla\Psi(t, u; \epsilon)$ has at least N periodic solutions contained in D_R. Particularly, the flow induced by system (1) with T-periodic protocol $z_\epsilon(t)$ has infinity many periodic trajectories with zero winding number.*

Proof. The spirit of this proof is to use Theorem 3.1 in a certain period annulus where the regularity hypotheses are satisfied. First, since the outer boundary of the whole period annulus of the center in system (3) is a saddle connection, the period of the periodic orbits tends to infinity as they approach the outer boundary. Second, setting $p = (x^*, 0)$ the center itself, Lemma 3.2 states that the period tends to

$$T_0(x^*) = \frac{2\pi}{\sqrt{\theta_0^2 \nu(\frac{x^*}{R})(2 + \nu(\frac{x^*}{R}))}}$$

as the orbits tends to p. The analyticity of the period function ensures then that for any $M > 0$ large enough there exists a period annulus, namely $\mathcal{A}_M$, such that the period of its orbits covers $[T_0(x^*), M]$.

Let us apply Theorem 3.1 in $\mathcal{A}_M$. To this end, it is enough to show that $\nabla\Psi(t, \eta; \epsilon)$ is continuous in $(t, \eta; \epsilon) \in \mathbb{R} \times \mathcal{A}_M \times (0, \epsilon_0)$ for some $\epsilon_0 > 0$, locally Lipschitz continuous in $\eta = (x, y) \in \mathcal{A}_M$ and T-periodic in t. From the expression in (10),

$$\nabla\Psi(t, \eta; \epsilon) = \begin{pmatrix} -y\theta_0 + c\theta_0 y \left(\dfrac{1}{(x - r_\epsilon(t))^2 + y^2} - \dfrac{1}{(x - \frac{R^2}{r_\epsilon(t)})^2 + y^2} \right) \\ \theta_0 x - c\theta_0 \left(\dfrac{x - r_\epsilon(t)}{(x - r_\epsilon(t))^2 + y^2} - \dfrac{x - \frac{R^2}{r_\epsilon(t)}}{(x - \frac{R^2}{r_\epsilon(t)})^2 + y^2} \right) \end{pmatrix}.$$

First, we claim that $\lim_{\epsilon \to 0} r_\epsilon(t) = r_0$ uniformly on $t \in \mathbb{R}$. Indeed, it follows from the definition of $r_\epsilon(t)$ and the fact that f is bounded. Second, we notice that $(r_0, 0) \notin \mathcal{A}_M$ since the period of the periodic orbits surrounding the vortex $(r_0, 0)$ tends to infinity as they approach the vortex. Consequently,

$$\liminf_{\epsilon \to 0} d(\mathcal{A}_M, r_\epsilon(\mathbb{R}) \times \{0\}) > 0$$

since $\mathcal{A}_M$ is a compact set. This checks the continuity of the map $\nabla\Psi$. Moreover, $\nabla\Psi(t, \cdot; \epsilon) \in C^1(\mathcal{A}_M)$ so also the property of being locally Lipschitz continuous in $\mathcal{A}_M$ holds. Then we are in position to apply Theorem 3.1 and, particularly, Corollary 1 and show that for any positive integer N there exists $0 < \bar{\epsilon}_N < \epsilon_0$ such that if $|\epsilon| < \bar{\epsilon}_N$ then system $\dot{\eta} = J\nabla\Psi(t, \eta; \epsilon)$ has at least N periodic solutions in $\mathcal{A}_M \subset D_R$. Finally, by construction of $\mathcal{A}_M$ those periodic solutions have zero winding number with respect to the vortex. $\square$

4. **Conclusions.** The main result of Section 2 has a natural reading for the underlying physical model. Note that ρ_0 is the ratio between the path and domain radii respectively, while ϕ_0 measures the relation between the path angular speed and the vortex strength. The sign of ϕ_0 indicates if the sense of rotation of the vortex and the path is the same or opposite. For example, fixing the positive parameters R, Γ, r_0 and leaving θ_0, for small positive θ_0 there are no equilibria. Then, a first bifurcation point is $\theta_0^* = \frac{\Gamma}{2\pi R^2} \frac{R-r_0}{R+r_0}$, where a degenerate saddle appears at $(-R, 0)$. A second bifurcation point appears at $\theta_0^{**} = \frac{\Gamma}{2\pi R^2} \frac{R+r_0}{R-r_0}$. For $\theta_0 \in]\theta_0^*, \theta_0^{**}[$, there is a center and two hyperbolic saddles in the border of the domain connected by an heteroclinic. They travel along the border until they collide at $\theta_0 = \theta_0^{**}$ into a degenerate saddle, that enter into the domain as a hyperbolic saddle for values above θ_0^{**}. On the other hand, for negative values of θ_0, corresponding to opposite rotating sense of the vortex and the stirring protocol, we identify a typical saddle-node bifurcation.

In the bifurcation scheme identified in Section 2, saddles are connected by heteroclinic or homoclinic orbits that constitute barriers for the flux transport. Around the centers, the particles rotate with different periods, and this fact makes possible an application of a suitable result for perturbed Hamiltonians (see Section 3), proving that for a perturbed vortex path there exist infinitely many periodic solutions that do not rotate around the vortex.

Generically, one can expect that a perturbation of the vortex path will break the heteroclinic or homoclinic connections of the saddles giving rise to Smale horseshoes, a fact yet proven in some cases by Franzese and Zannetti in [6]. The problem to identify more general classes of vortex protocols that generate this kind of periodic orbits with zero winding number is still open. Also, the investigation of solutions of zero winding number in more general domains is an interesting open problem to be addressed in the future. Finally, from the analytical point of view little is known about the stability properties of the periodic trajectories in this context, the recent reference [7] goes on this direction.

REFERENCES

[1] H. Aref, Stirring by chaotic advection, *J. Fluid Mech.*, **143** (1984), 1–21.

[2] H. Aref, J. Roenby, M. A. Stremler and L. Tophøj, Nonlinear excursions of particles in ideal 2D flows, *Phys. D*, **240** (2011), 199–207.

[3] A. Boscaggin and P. J. Torres, Periodic motions of fluid particles induced by a prescribed vortex path in a circular domain, *Phys. D*, **261** (2013), 81–84.

[4] T. Carletti and A. Margheri, Measuring the mixing efficiency in a simple model of stirring: Some analytical results and a quantitative study via frequency map analysis, *J. Phys. A*, **39** (2006), 299–312.

[5] A. Fonda, M. Sabatini and F. Zanolin, Periodic solutions of perturbed Hamiltonian systems in the plane by the use of the Poincaré-Birkhoff Theorem, *Topol. Methods Nonlinear Anal.*, **40** (2012), 29–52.

[6] P. Franzese and L. Zannetti, Advection by a point vortex in closed domains, *European J. Mech. B Fluids*, **12** (1993), 43–67.

[7] R. Ortega, V. Ortega and P. J. Torres, Point-vortex stability under the influence of an external periodic flow, *Nonlinearity*, **31** (2018), 1849–1867.

[8] P. G. Saffman, *Vortex Dynamics*, Cambridge Monographs on Mechanics and Applied Mathematics, Cambridge University Press, New York, 1992.

[9] P. J. Torres, *Mathematical Models With Singularities*, Atlantis Briefs in Differential Equations, 1, Atlantis Press, Paris, 2015.

[10] S. Wiggins and J. M. Ottino, Foundations of chaotic mixing, *Philos. Trans. R. Soc. Lond. Ser. A Math. Phys. Eng. Sci.*, **362** (2004), 937–970.

E-mail address: david.rojas@udg.edu
E-mail address: ptorres@ugr.es